1983

Flow visualization study of natural convection from a heated protrusion in a liquid filled rectangular enclosure.

Knock, Rick Herman.

Monterey, California. Naval Postgraduate School

NAVAL POSTGRADUATE SCHOOL
Monterey, California

THESIS

FLOW VISUALIZATION STUDY OF NATURAL CONVECTION FROM A HEATED PROTRUSION IN A LIQUID FILLED RECTANGULAR ENCLOSURE

by

Rick Herman Knock

December 1983

Thesis Advisor: M. D. Kelleher

REPORT DOCUMENTATION PAGE

READ INSTRUCTIONS BEFORE COMPLETING FORM

1. REPORT NUMBER

2. GOVT ACCESSION NO.

3. RECIPIENT'S CATALOG NUMBER

4. TITLE (and Subtitle)
Flow Visualization Study of Natural Convection from a Heated Protrusion in a Liquid Filled Rectangular Enclosure

5. TYPE OF REPORT & PERIOD COVERED
Master's Thesis; December 1983

6. PERFORMING ORG. REPORT NUMBER

7. AUTHOR(s)
Rick Herman Knock

8. CONTRACT OR GRANT NUMBER(s)

9. PERFORMING ORGANIZATION NAME AND ADDRESS
Naval Postgraduate School
Monterey, California 93943

10. PROGRAM ELEMENT, PROJECT, TASK AREA & WORK UNIT NUMBERS

11. CONTROLLING OFFICE NAME AND ADDRESS
Naval Postgraduate School
Monterey, California 93943

12. REPORT DATE
December 1983

13. NUMBER OF PAGES
69

14. MONITORING AGENCY NAME & ADDRESS(if different from Controlling Office)

15. SECURITY CLASS. (of this report)
Unclassified

15a. DECLASSIFICATION/DOWNGRADING SCHEDULE

16. DISTRIBUTION STATEMENT (of this Report)
Approved for public release; distribution unlimited.

17. DISTRIBUTION STATEMENT (of the abstract entered in Block 20, if different from Report)

18. SUPPLEMENTARY NOTES

19. KEY WORDS (Continue on reverse side if necessary and identify by block number)
Natural Convection
Rectangular Enclosure
Flow Visualization

20. ABSTRACT (Continue on reverse side if necessary and identify by block number)

A flow visualization study of natural convection in a liquid filled rectangular enclosure with a small heater protruding into it from one vertical wall was conducted. The top and bottom horizontal surfaces of the enclosure were heat exchangers whose temperatures could be varied independently. The fluid in the enclosure was water. The Baker electrochemical technique which utilizes a pH indicator was

used for flow visualization. Photographs were taken of the two dimensional flow for three different locations of the heater on the vertical wall. Nusselt numbers for each heater location and for a range of Rayleigh numbers were also determined. Visual results indicate the presence of a dual-cell configuration within the enclosure. There is a buoyancy driven upper cell and a shear driven lower cell. The flow of the upper cell follows the geometry of the enclosure. Though the uncertainty inherent in the experiment was high data calculations suggest a trend that as the heater is raised within the enclosure the Nusselt number decreases.

Approved for public release; distribution unlimited.

Flow Visualization Study of Natural Convection from a Heated Protrusion in a Liquid Filled Rectangular Enclosure

by

Rick Herman Knock
Lieutenant Commander, United States Navy
B.A., Albion College, 1972

Submitted in partial fulfillment of the requirements for the degree of

MASTER OF SCIENCE IN MECHANICAL ENGINEERING

from the

NAVAL POSTGRADUATE SCHOOL
December 1983

ABSTRACT

A flow visualization study of natural convection in a liquid filled rectangular enclosure with a small heater protruding into it from one vertical wall was conducted. The top and bottom horizontal surfaces of the enclosure were heat exchangers whose temperatures could be varied independently. The fluid in the enclosure was water. The Baker electrochemical technique which utilizes a pH indicator was used for flow visualization. Photographs were taken of the two dimensional flow for three different locations of the heater on the vertical wall. Nusselt numbers for each heater location and for a range of Rayleigh numbers were also determined. Visual results indicate the presence of a dual-cell configuration within the enclosure. There is a buoyancy driven upper cell and a shear driven lower cell. The flow of the upper cell follows the geometry of the enclosure. Though the uncertainty inherent in the experiment was high data calculations suggest a trend that as the heater is raised within the enclosure the Nusselt number decreases.

TABLE OF CONTENTS

LIST OF TABLES

LIST OF FIGURES

NOMENCLATURE

Symbol	Description	Units
A	Area	in^2 or ft^2
g	Acceleration of gravity	Ft/sec^2
Gr	Grashof number	Dimensionless
h	Convection heat transfer coefficient	$Btu/hr\text{-}ft^2\text{-}^oF$
k	Thermal conductivity	$Btu/hr\text{-}ft\text{-}^oF$
k_f	Fluid thermal conductivity	$Btu/hr\text{-}ft\text{-}^oF$
k_g	Thermal conductivity of plexiglas	$Btu/hr\text{-}ft\text{-}^oF$
k_i	Thermal conductivity of foam rubber insulation	$Btu/hr\text{-}ft\text{-}^oF$
k_p	Thermal conductivity of phenolic	$Btu/hr\text{-}ft\text{-}^oF$
k_{ss}	Thermal conductivity of 304 stainless steel	$Btu/hr\text{-}ft\text{-}^oF$
L	Characteristic length	Inches
Nu	Nusselt number	Dimensionless
Pr	Prandtl number	Dimensionless
Q_{cond}	Heat loss via conduction through vertical walls	Btu/hr
Q_{conv}	Energy convected into fluid from heater	Btu/hr
Q_{in}	Energy into cartridge heater	Btu/hr
R	Resistance of precision resistor	Ohms
Ra	Rayleigh number	Dimensionless

R_a	Equivalent thermal resistance to conduction through viewing wall	Hr-^oF/Btu
R_b	Equivalent thermal resistance to conduction through wall opposite viewing wall	Hr-^oF/Btu
R_c	Equivalent thermal resistance to conduction through wall holding heater	Hr-^oF/Btu
R_{cond}	Total thermal resistance to conduction with respect to heat loss through vertical walls	Hr-^oF/Btu
R_j	Individual thermal resistance to conduction (j=1,7)	Hr-^oF/Btu
T_a	Ambient temperature	^oF
T_f	Average temperature of heat exchangers	^oF
T_h	Cartridge heater temperature	^oF
T_i	Thermocouple temperatures (i=1,8)	^oF
T_s	Average temperature of heater	^oF
V_1	Voltage across heater	Volts
V_2	Voltage across precision resistor	Volts
W	Uncertainty of variables	Various
α	Thermal diffusivity	Ft^2/sec
β	Coefficient of expansion	1/^oF
ν	Kinematic viscosity	Ft^2/sec

ACKNOWLEDGEMENT

The author would like to express his deep gratitude to Professor M. D. Kelleher, his thesis advisor, for his guidance and advice in this endeavor.

He wishes to express appreciation to Mr. Charles Crow of the Mechanical Engineering Department for his excellent work in manufacturing the flow visualization apparatus.

The author would like to thank the Educational Media Department photography lab personnel for their continual effort in developing all photographs.

Last but not least, a special word of thanks and sincere appreciation to my wife, Linda, whose understanding and patience allowed completion of this task in a timely manner.

I. BACKGROUND

A. INTRODUCTION: STATEMENT OF PROBLEM

The rapid advancements in the field of miniaturization of electronic components is well-known. Technology has brought us from the large-scale integration (LSI) device to the very large-scale integration (VLSI) device in just a few short years. Since the first 1 kilobit RAM semiconductor device was introduced in 1970 the number of memory cells on a single device has grown to 64K while the size of the device has decreased. One such device, the 64K RAM Micron chip produced by Tiny Micron Technology, Inc. is only 22,000 square mils, or approximately the size of one of these printed letters [1]. Yet microminiaturization advancements are far from over -- 256K and greater RAM chips are on the immediate horizon.

As in most rapidly developing technologies there are various problems associated with the advancements that have been made in the miniaturization of electronic devices. One of the primary problems that has evolved is that of suitably cooling components so that they will perform reliably over long periods of time. For though the size of the individual component has shrunk considerably its junction temperature has remained fairly constant. It follows that the decrease in device size has been kin to an increase in heat flux.

To get an idea of the magnitude of this decreased size/increased heat flux relationship one only has to heed the words of Chu [2]. He asserts that the heat flux of a microcircuit chip is but two orders of magnitude less than the heat flux of the sun (10^5 vice 10^7 Watts per meter squared). Further, the microcircuit chip must dissipate its energy at strict maximum junction temperatures of between 125 to 150 degrees C. The integration of a multitude of devices on a single printed circuit board leads to an increase in the temperatures in which the device operates. The high heat flux of the microcircuit chip coupled with the increase in environmental temperature very often leads to the problem of component failure resulting from inadequate cooling. It is this problem that has recently prompted extensive research into the techniques of cooling microelectronic devices.

B. DESIGN CONSIDERATIONS: PROPOSED SOLUTIONS

Many papers have been published outlining alternative methods of thermally controlling microelectronic devices. Hannemann [3] describes the thermal considerations that must be taken into account at each level (subassembly, assembly, and system levels) of the device design process. Kraus, et al [4] assert the need for thermal analysis even after design. They propose a strategy that yields conservative estimates of the heat flux associated with electronic circuitry. Further, Bar-Cohen, et al [5] indicate that numerical

analysis of the heat transfer problem should be relied upon to cope with the analytically intractable nature of even standard packaging configurations.

Once the initial design step has been completed a reliable cooling scheme must be employed. A number of such schemes including conduction, forced air cooling, and direct liquid cooling have been proposed by many authors. Bergles, et al [6] contend that of the many techniques available, direct liquid cooling may be the most desirable mode of heat transfer when considerations such as weight, size, or cost are taken equally into account with the heat transfer coefficient. Simons and Moran [7] support this view by stating that liquid coolants offer the capability to achieve heat transfer coefficients one to two orders of magnitude higher than that of air.

Many authors have offered alternative methods of utilizing immersion cooling. One such scheme is proposed by Kraus and Bar-Cohen [8] who analyze submerged condensers. They describe a model whereby the heat from the immersed electronic devices is removed via bubble pumped augmented convection interacting at the submerged condenser surface.

This study focuses on direct liquid cooling by natural convection. More specifically, since most microelectronic devices are seated on printed circuit boards packaged very near each other, investigation is limited to natural convection in a small liquid filled rectangular enclosure. One

advantage of natural convection cooling is that there are no pumps, pipes, or any other equipment within the enclosure; the manufacture of a relatively small module may be assured.

C. IMMERSION COOLING: ANALYTICAL STUDIES

Numerous analytical studies of natural convection in rectangular enclosures have been made since 1966 when Wilkes and Churchill [9] initiated finite difference analysis for such configurations. This work was followed by many others including Szekely and Todd [10] who, in 1970, presented a finite difference analysis of natural convection in a rectangular cavity in which two opposing vertical walls provide the temperature gradient. Comparing their numerical results with experiment they concluded that within the Rayleigh number range of sixteen hundred to sixty-thousand the thermal response of a system is approximately independent of the Rayleigh number. They further noted a trend for secondary cells to develop once the Rayleigh number exceeded three hundred thousand.

In 1975 Chu, et al [11] studied, via finite difference methods and experiment, the natural convection in a rectangular enclosure in which the heat source was a long, horizontal strip located in one vertical wall. Focusing on heater location, heater size, and enclosure size a conclusion was reached that as the Rayleigh number increases the heater location for maximum circulation shifts downward but

that heater size seems to have little effect on circulation. They contend that secondary cells develop at the upper surface as the height of the enclosure is increased.

Markatos and Pericleous [12] have recently published a study of buoyancy-driven flow in a square cavity with differentially heated sides. Secondary cells were also observed in their study.

D. IMMERSION COOLING: EXPERIMENTAL STUDIES

Megerlin and Vingerhoet [13] collected natural convection data using fluorocarbon dielectric fluids in an enclosure modeled after a microelectronic module. One significant conclusion reached was that cold plate orientation has a significant effect on the heat transfer -- a fifty percent increase is attained using a horizontal vice vertical cold plate. An experimental investigation using an undivided and partially divided water filled two-dimensional rectangular enclosure was performed by Nansteel and Greif [14].

In 1972 Baker [15] published the results of his experimental work in which he used resistors immersed in Freon. He concluded that the heat dissipation obtained with Freon is at least four times greater than that obtained using the same assembly with stagnant air. Lin and Akins [16] investigated natural convection heat transfer in a fluid filled cube where all six wall temperatures were subjected to a step change in temperature. Their conclusion was that a variety of circulation patterns evolve depending on the size of the cube.

In 1980 Ostrach, et at [17] published the results of an experiment that used small particles introduced in silicone oils that filled various sized rectangular enclosures with height to length ratios less than unity. Secondary cells were evident in their study. Finally, an experiment was performed by Bohn and Kirkpatrick [18] which studied high Rayleigh number natural convection in a cublical enclosure filled with deionized water using various combinations of heated walls. They concluded that heating from below along with simultaneous vertical wall heating and cooling enhances heat transfer.

The above discussion is not intended to be a definitive synopsis of all works in the design considerations of microelectronic devices, nor in the numerical analysis and experiments conducted on natural convection in enclosures. References cited are merely intended to be representative of the works that have been done in these areas. They serve to provide an excellent point of departure for the remainder of this study. For a more extensive review of the works done concerning natural convection in rectangular enclosures the reader is referred to Catton [19].

E. OBJECTIVES

The objectives of this study are:

1. to design and build an apparatus that approximates a liquid filled microelectronic package with appropriate printed circuit board spacing that is cooled by heat exchangers acting

as the top and bottom horizontal surfaces. The heat source is to be a rectangular protrusion modeled geometrically after a 40-pin dual-in-line package (DIP) that is attached to and horizontally traverses the length of one vertical wall.

2. to observe the steady state natural convection flow in the apparatus using a variety of heater and heat sink temperatures as well as various locations of the heating element.

3. to analyze data obtained and determine Nusselt and Rayleigh numbers for each apparatus configuration.

This study is intended to serve as a basis for future heat transfer experiments in natural convection using various enclosure sizes and multiple heated protrusions.

II. EXPERIMENT

A. GENERAL DESIGN CONSIDERATIONS

The flow visualization apparatus (Fig. 1) consists of a small liquid filled rectangular enclosure with a heater modeled geometrically after a 40-pin DIP protruding into the enclosure from one of the vertical walls. This configuration is meant to simulate a microelectronic component on a printed circuit board. The top and bottom horizontal surfaces of the enclosure are such that their temperatures can be varied independently. Heat exchangers (Fig. 2) used in conjunction with a circulating bath act as these horizontal surface. A cartridge heater housed in a stainless steel cover (Fig. 3) acts as the 40-pin DIP model. This assembly is hereafter referred to as the heater. A calibrated resistor put in series with the heater and its power supply allows the input power to be accurately determined. Eight thermocouples are placed throughout the enclosure for temperature measurements. Two are placed on each heat exchanger and four on the cartridge heater cover.

Several criteria were established to be used as guidelines for design. The following is a list of these criteria and their implications.

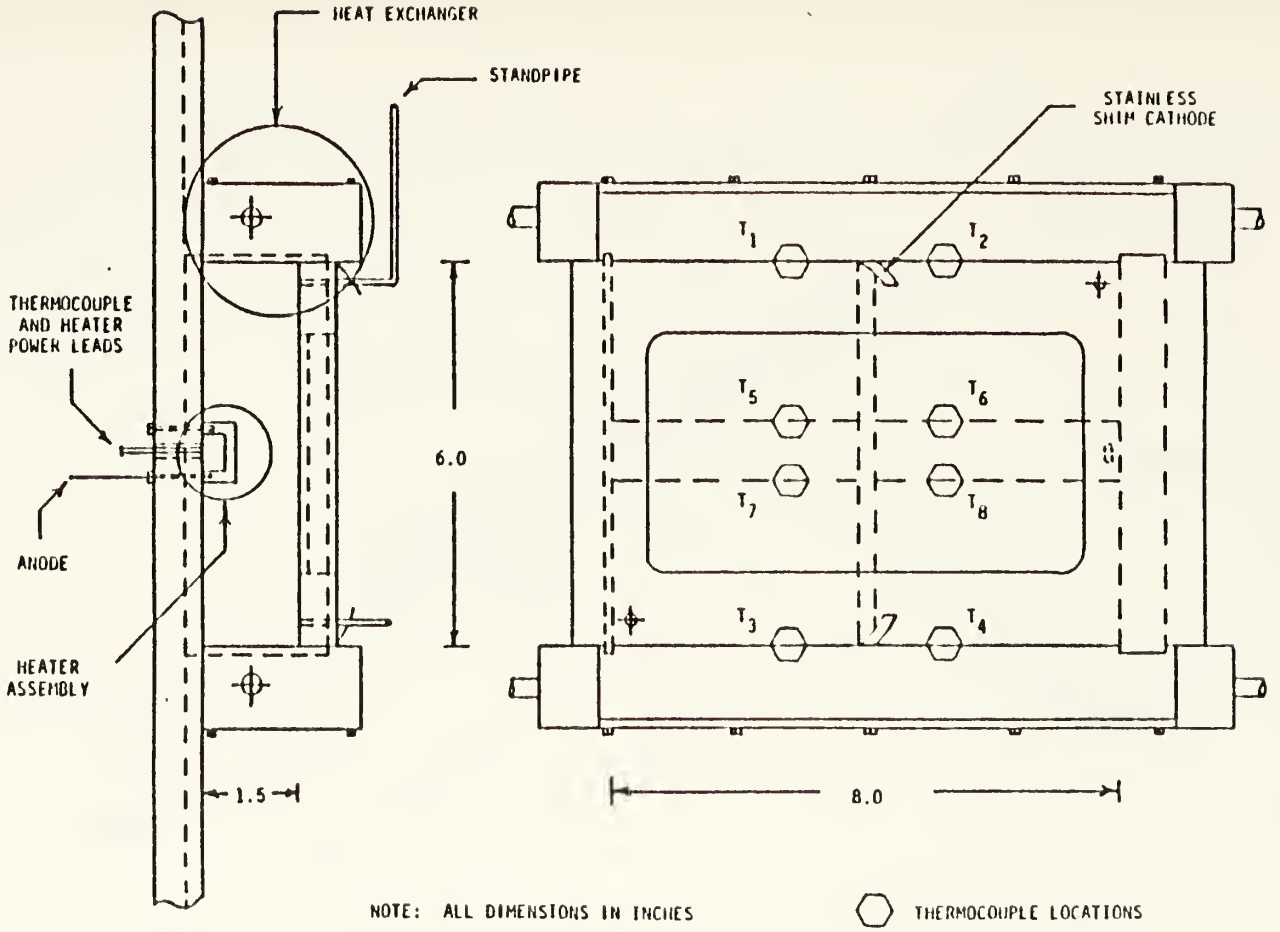

Figure 1. Test Chamber

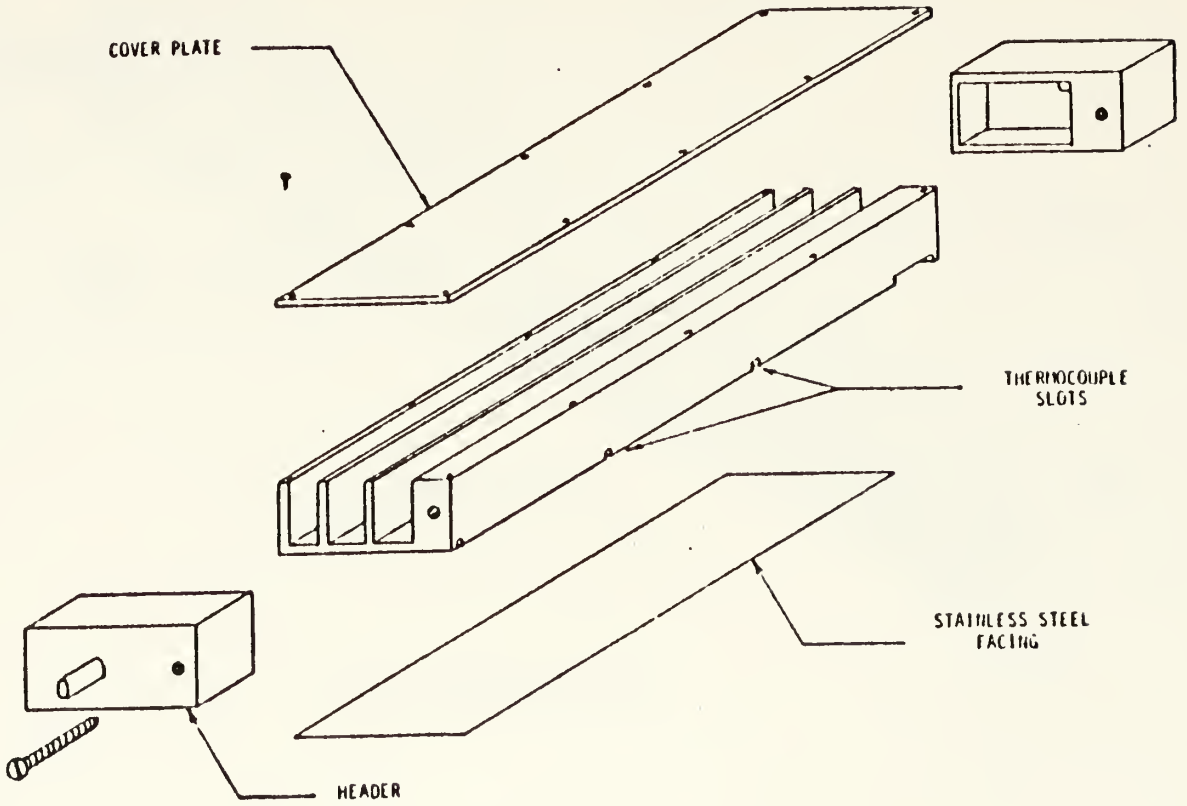

Figure 2. Heat Exchangers

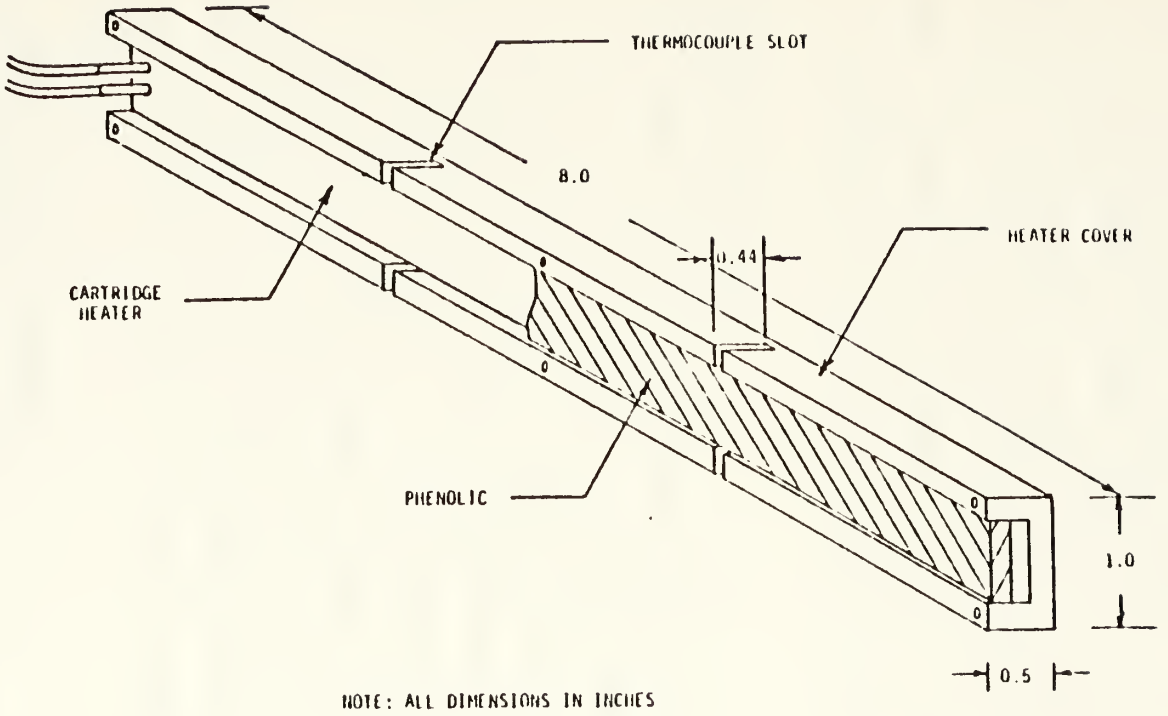

Figure 3. Heater Assembly

1. Dimensions

As previously noted, the heater was to model geometrically a 40-pin DIP. Micrometer measurements of the height and width of a packaged 40-pin DIP were made and the rectangular heater cover is made to approximate these dimensions. Further, the enclosure's height was to be 6 times the vertical dimension of the heater cover and its width was to be between 3 and 4 times the heater cover's horizontal dimension. This provides a good approximation to the spacing of a vertical printed circuit board placed in an electronic module.

2. Heater Location

The apparatus was to be made such that the heater could be raised or lowered on the vertical wall and that the width of the enclosure could be made to vary from 1 to 2 inches. This would provide a wide range of enclosure sizes and heater locations for investigation. It was determined that the ability to move the vertical wall on which the heater is attached is better for preserving fluid-tight integrity and smoothness. Machine milled interconnecting parts are successfully used to meet this and the variable chamber width requirements.

3. Visualization Technique

The thymol-blue pH indicator flow visualization technique proposed by Baker [20] was to be used. This is a non-intrusive technique that uses a pH indicator in distilled

water. When a voltage is applied across the fluid it perceptibly darkens near the negative electrode due to a local change in pH induced by proton transfer. If there is fluid motion away from the cathode, as there is in this experiment, the darkened fluid traces the path of motion before dissipating back to the original lighter color and neutral pH of the bulk fluid. In addition to its non-intrusive quality no density differences occur within the fluid during voltage application since the pH indicator remains an ion in solution. The specifics of the fluid preparation are discussed in Chapter III. After much testing it was determined that the use of this technique requires any metal coming into contact with the liquid solution (e.g., heat exchangers, heater) to be relatively inactive with respect to the Galvanic series. This prevents corrosion as indicated by O'Conner [21]. To this end, a stainless steel shim strip running the length of the vertical wall opposite the heater is used as the cathode. The heater acts as the anode. This arrangement provides excellent visualization of the two dimensional flow of the darkened solution.

4. Other Considerations

One eighth inch plexiglas is used as the vertical viewing wall to minimize optical distortion. Further, all vertical walls are heavily wrapped with foam rubber insulation to minimize heat loss via conduction through them during experimental operation.

B. COMPONENTS

1. Heater

The heater assembly (Fig. 3) consists of an 8 inch long, 1/2 inch wide, 1 inch high, and 3/16 inch thick 304 stainless steel channel that houses a narrow rectangular cartridge heater backed by phenolic insulation that runs the length of the channel. The cover has four 1/16 inch deep slots located on the horizontal faces 2.75 inches from the ends of the channel. In each of these slots a copper-constantan thermocouple is spot welded nearest the cover's vertical face. The thermocouple wires run out the back of the slots into the channel. The slots are filled with steel epoxy. Three evenly spaced screw holes are tapped into the top and bottom of the cover so that the entire assembly can be attached to a vertical wall in the enclosure. Prior to installation the cover is polished to a mirror-like finish using 180 to 600 grit special silicon carbide grinding paper and then cleaned with common rubbing alcohol.

2. Heat Exchangers

The two aluminum heat exchangers measure 1.5 by 2.5 by 11.0 inches. The top heat exchanger is seen in Fig. 2. They each have three rectangular channels separated by 1/8 inch walls. The channels are machine milled into a 1.375 by 2.5 by 9.25 inches solid piece of stock aluminum and then covered with a 1/8 inch thick plate secured by ten no. 4 screws. Slots 1/8 inches deep are milled 8.0 inches apart

on the side opposite the cover plate to accept vertical walls. One slot is 3/16 inches in width and the other 3/4 inches in width. Both slots traverse the width of the heat exchanger. In addition, two 1/16 inch deep slots are milled 2.75 inches from the outer slots and they run to within 1 inch of the other side of the exchanger. These last two slots have copper-constantan thermocouples spot welded into them and are covered with steel epoxy. A 1.5 by 8.0 inch 0.001 gage stainless steel shim facing is epoxied in between the two outer slots on the side of the exchanger opposite the cover plate. It is positioned flush against the corner of the heat exchanger that is one inch from the thermocouple slots. This facing is the relatively inactive portion of the exchanger that acts as the horizontal wall of the chamber.

The 1.5 by 2.5 by 0.875 inch headers are also machined from single pieces of aluminum stock. They each have a 1/4 inch od, 1/8 inch id exterior pipe for coupling with a circulating bath and a 2 square inch hollow interior positioned so as to get maximum flow in each exchanger channel. The headers are held to the main body of the exchangers by a single no. 6 screw. All seams are fitted with epoxy prior to assembly.

Both heat exchangers were tested for temperature distribution and leakage prior to use in the experiment. They were coupled to a circulating bath and temperature measurements were taken using the two installed thermocouples

and an additional similar thermocouple that was randomly moved about the exchanger surface. The thermocouples were run to a digital pyrometer with an accuracy of 1 degree Fahrenheit. It was determined from this test that the heat exchangers are, upon reaching steady state, at a constant temperature throughout; i.e., the pyrometer reading was the same for each thermocouple.

3. Test Chamber

The test chamber seen in Fig. 1 forms a rectangular enclosure measuring 1.5 inches in width, 8.0 inches in depth, and 6.0 inches in height. The top and bottom horizontal surfaces of the enclosure consist of the stainless steel shim facing of the heat exchangers. Three of the vertical walls are entirely plexiglas. The wall holding the heater is 10.5 inches wide, 24 inches high, and 11/16 inches thick. The heater is secured to the center of this wall with six no. 4 screws and rubber o-rings that are counter sunk into the wall. In addition, a 1/2 inch diameter hole is located 1 inch from one end of the wall to accommodate the cartridge heater power leads and thermocouple wires from the heater cover. The wall has two 1/4 inch deep slots, one 3/16 inches in width and the other 3/4 inches in width, 8 inches apart and 14 inches long running parallel along its height. These slots receive the adjacent vertical walls. They also allow the wall and subsequently the heater to be raised or lowered while maintaining fluid tight integrity.

The other two plexiglas vertical walls are the ends that comprise the 1.5 by 6.0 inch dimensions of the enclosure. They are both 2 inches by 6.25 inches but one is 11/16 inches thick while the other is 1/8 inches thick. The thinner wall is used for visualization and photography and was chosen to be thin in order to minimize optical distortion. Both walls slide into the 1/4 inch slots of the two larger adjacent walls and into the 1/8 inch deep slots on the heat exchangers.

The final vertical wall of the enclosure is a 10.0 inch by 6.0 inch plexiglas frame that house a glass plate. The plate is installed with epoxy and will be used for future studies in conjunction with laser doppler velocimetry. Like the other large wall it has two 1/8 inch deep slots that receive the adjacent walls. The wall has lips that slide into the heat exchanger slots as well as two 1/16 inch id standpipes made of 1/8 inch stainless steel tubing. One standpipe is located near an upper corner and the other is diagonally opposite. They are used for filling/emptying the enclosure and relieving internal pressure during experimental operation.

C. ASSEMBLY

Once the heater has been attached to the large wall the apparatus is assembled with the exception of the glass wall framed by plexiglas. Dow Corning 732 RTV adhesive/sealant is applied externally to all seams not involved with visualization, to the power lead/thermocouple hole, and to the heads

of all heater attaching screws. A thin coat of Dow Corning 3140 RTV coating and silastic is used on all internal seams and on all of the external seams of the smaller walls. The glass wall framed by plexiglas is then fitted into place along with a taut 1/4 inch wide strip of 0.001 gage 302 stainless steel shim. The strip is centered internally on the wall and runs its height. A few inches of the strip traverse the seams between the wall and the heat exchangers (both top and bottom) to the outside of the test chamber. This strip acts as the cathode for the thymol-blue visualization technique. The sealants are then applied to all remaining seams and the apparatus is tightened by specially made clamps. Fig. 4 is a photograph of the assembled apparatus.

The vertical wall of the apparatus that holds the heater has to be removed, placed at the desired heater height, and then resealed between test runs. If removing the wall between test runs is not desired the apparatus can be turned upside-down to attain a different heater height.

D. INSTRUMENTATION

1. Power to the Heater

The heater is run in series with a precision resistor that was measured to have a 2.0317 ohms resistance on a Rosemount commutating galvonometer bridge. This arrangement allows a voltage measurement across the resistor to be made and, using its known resistance, the current through the

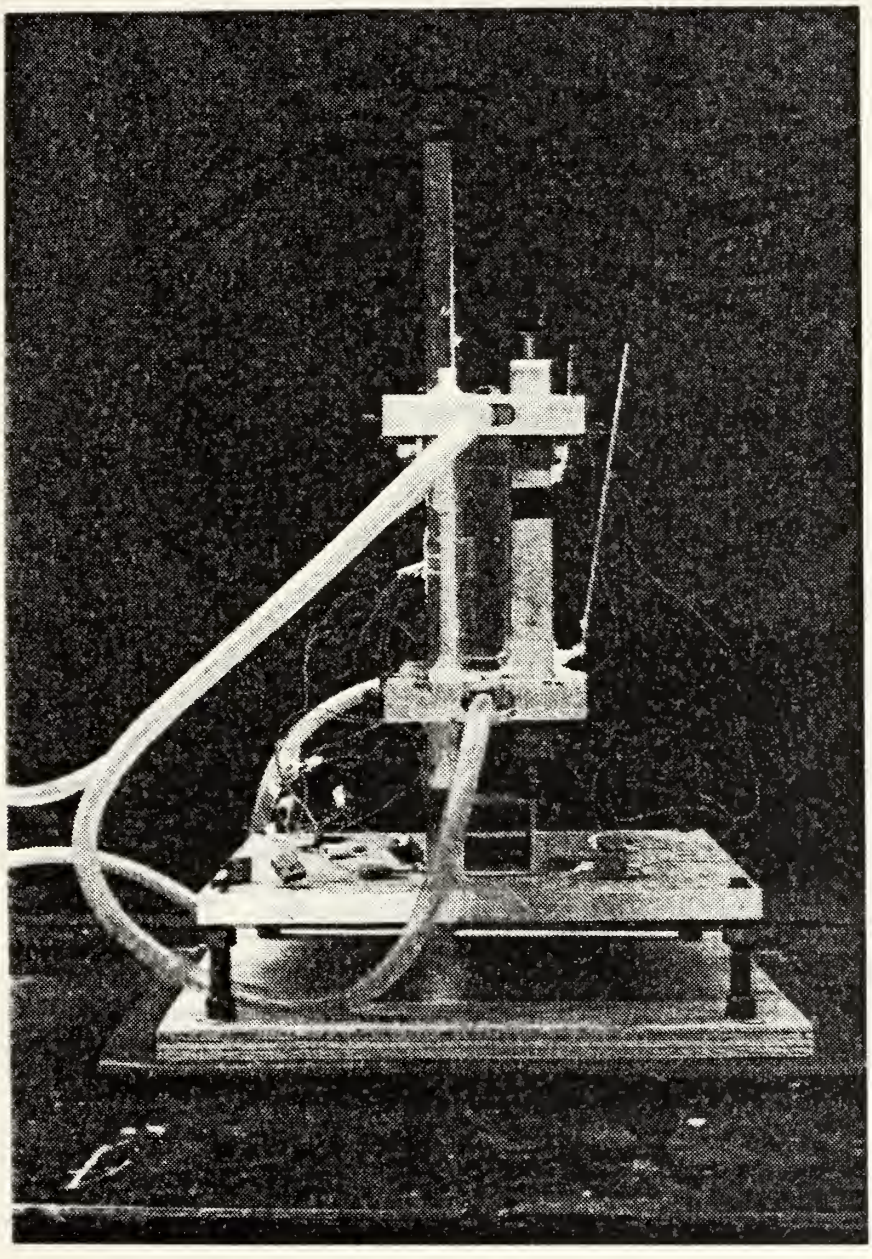

Figure 4. Photograph of Experimental Apparatus

circuit can be calculated. A measurement of the voltage across the heater is also taken. The product of the current and the voltage across the heater gives input power to the heater. Both voltages are measured using a Dana digital multimeter.

Because of the 180 watt, 120 volt rating of the cartridge heater two different power supplies are used in order to attain certain voltage levels. A Lambda regulated DC power supply is used for voltages up to 60 volts. A Variac voltage AC transformer is used for voltages greater than 60 volts. A concern about using the latter was the fluctuating voltage provided by house current and its possible effect on measurements. As it happened, temperature measurements remained stable. However, voltage measurements across the heater fluctuated up to 3.0%. Subsequently, calculations of input power to the heater are less accurate with this mode of operation than the power calculations made when the Lambda regulator is used. A better method when using the Variac would have been to put it in series with a line voltage regulator in order to eliminate voltage fluctuations caused by house current.

2. Voltage Across the Fluid

The voltage source for the electrochemical technique is also a Lambda regulated DC power supply. Voltages across the electrodes range from 3.0 to 8.0 volts depending upon the contrast of the fluid required for photography. The

voltage is measured with the Dana digital multimeter. The stainless steel shim strip running the height of the vertical glass wall framed by plexiglas acts as the cathode while the stainless steel heater cover acts as the anode. Electrical access to the heater cover is via a wire spot welded to the bottom center stainless steel attaching screw that holds the heater assembly to the vertical wall opposite the cathode.

Originally the heater was utilized as the anode and the top heat exchanger acted as the cathode. This arrangement proved unacceptable because flow paths could not easily be discerned from the viewing perspective. The inclusion of the shim strip as the cathode solved this problem by limiting the darkened flow to a single path located in the center of the enclosure.

3. Temperature Measurement

Eight, 30 gage copper-constantan (teflon/teflon insulation) thermocouples dispersed throughout the enclosure are used for temperature measurements. Two thermocouples are located on each horizontal face of the heater cover and two on each heat exchanger. All thermocouples were fabricated using a Dynatech welder and calibrated on a Rosemount commutating bridge in conjunction with a platinum resistance temperature standard and calibration bath.

The thermocouples run to a Newport digital pyrometer model 267 where temperature readings are made. The pyrometer

gives readings to the nearest degree Fahrenheit. If, during the measuring process, a reading fluctuates between two temperature extremes it is assumed to be the average of the two. Finally, the ambient temperature is measured within two feet of the apparatus with another thermocouple run to the pyrometer.

III. EXPERIMENTAL PROCEDURE

A. ELECTROCHEMICAL FLUID PREPARATION

As noted earlier, the thymol-blue pH indicator flow visualization technique as described by Baker [20] is used. Further, O'Conner suggests using thymol-blue sodium salt vice pure thymol-blue (thymolsulphonephthalein) crystals in the solution to avoid filtering of undissolved crystals [21]. This advice is followed in the preparation of the fluid. First, 0.2 grams of thymol-blue sodium salt are dissolved in 1.0 liter of distilled water. This gives a 0.02% by weight light colored solution with no undissolved solids. Next, 0.1 normal sodium hydroxide is added drop by drop to the solution until it titrates to a dark blue color. The dark color is an indication of a slightly basic pH. Finally, the solution is titrated back to its original lighter color by adding drop by drop 0.1 normal hydrochloric acid. The fluid is now slightly acidic and very close to its neutral pH value of 7. After preparation, a small amount of fluid is poured into a shallow glass container. Wires attached to a 1.5 to 7.5 volt dry cell battery are used as the electrodes and the fluid is tested for local color change. All tests indicate adequate color change.

B. APPARATUS PREPARATION

After the sealants are cured, 1/4 inch tygon tubing is attached to the heat exchangers using stainless steel hose clamps. The exchangers are then interconnected in series to a refrigerated circulating bath placed six feet from the apparatus. The top heat exchanger is placed upstream of the bottom exchanger. Common tap water is used as the refrigerated circulating coolant. The apparatus is then laid horizontally on its largest wall. 1.5 feet of 1/8 inch tygon tubing is attached to each standpipe and the enclosure is filled with the thymol-blue solution via a simple siphon system. Manual manipulation of the apparatus and standpipe tubing allows most bubbles to be driven out of the enclosure.

A specially made steel leveling stand with four height adjustable legs and a slot for the largest vertical wall had been made to hold the apparatus. The stand is placed on a piece of plywood under which lies two inches of foam rubber insulation. This system serves to damp out any vibrations occurring in the laboratory. The apparatus is placed vertically upright onto the leveling stand and secured in place. The two larger vertical walls are then layered with 3/4 inch thick insulation. After insuring that the view through the test chamber to a white background is unobstructed, 3/4 inch thick insulation is placed on the remaining vertical walls. The apparatus is then leveled both horizontally and vertically by means of a bubble level placed on the top heat exchanger

in two orthogonal directions and by concurrent adjustment of the stand legs. This leveling process is crucial for ensuring horizontal and vertical alignment of the chamber. Fig. 5 is a photograph of the assembled apparatus and instrumentation.

C. TEST PROCEDURE

1. Heater Location

Test runs were made for three heater locations: (1) the top horizontal face of the heater located 1.0 inch from the top of the enclosure, (2) the heater centered on the vertical wall of the enclosure, and (3) the bottom horizontal face of the heater located 1.0 inch from the bottom of the enclosure.

2. Initial Instrument Settings

Temperature measurements of all thermocouples are made to insure that the apparatus and its liquid contents are at a single temperature. If this criteria is met the circulating bath to the heat exchangers is turned on to a predetermined temperature. Shortly thereafter the power supply to the heater is turned on and the voltage slowly increased to another predetermined value that results in the approximate desired temperature difference between the exchangers and the heater. The values of the settings for the circulating bath temperature and the voltage to the heater are determined soley from experience garnered from a multitude of test runs.

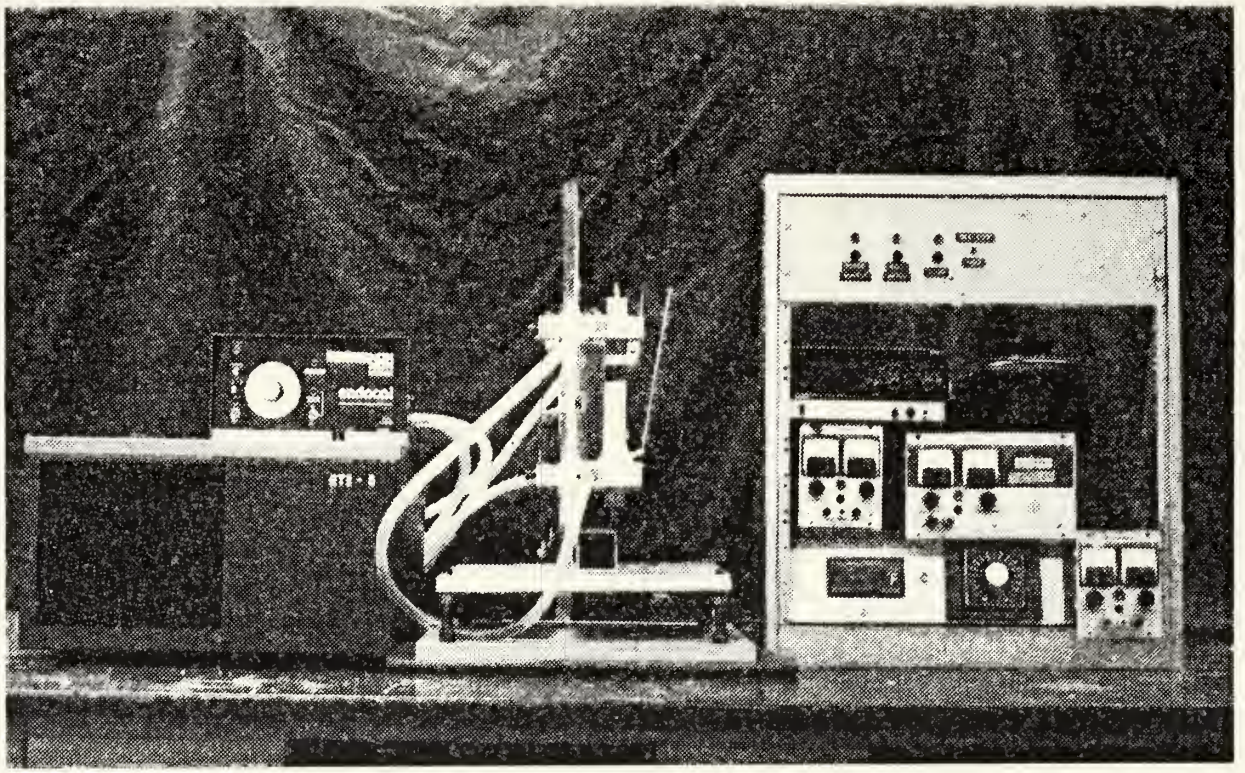

Figure 5. Photograph of Experimental Apparatus and Instrumentation

3. Instrument Readings

Thermocouple temperature measurements and voltage measurements across the heater and resistor are taken every twenty minutes until successive temperature measurements remain unchanged to within the accuracy of the pyrometer. Measurements are then taken every ten minutes. It is assumed that steady state is attained within the enclosure if no thermocouple measurement changes by more than one degree during any ten minute period. This process takes between two to four hours depending on the initial temperature difference between the heater and the exchangers. The smaller temperature difference takes the least amount of time.

Once steady state is attained the power supply that creates the voltage across the electrochemical fluid is turned on. Using a digital multimeter as an indicator, the voltage is increased from 0.0 to 3.0 volts. The insulation is then removed from the two smaller vertical walls and the fluid voltage is varied until a visually suitable path of darkened fluid ensues.

4. Photographic Techniques

A Nikon Ftn with a 50 mm f2 lens is used for all black and white photography. A Canon Ftb with a 50 mm f1.4 lens is used for all color photography. Black and white photographs are taken with Kodak Tri-x pan asa 400 film; color photographs are taken with Kodak Ektachrome asa 64 daylight film. Black and white photographs are taken first. Both

cameras are secured to a tripod. The Nikon is placed between 14 and 15 inches from the 1/8 inch thick plexiglas vertical wall. A combination of f-stop settings of 8 and 11 coupled with shutter speeds of 1/60 and 1/125 of a second are used. The Canon is placed at a distance of between 12 and 13 inches from the viewing wall. Combinations of f-stop 2 and 4 with shutter speeds of 1/4 and 1/15 of a second are used with the Canon.

Two L-shaped pieces of cardboard are attached together so as to create a rectangular opening approximately the size of the small vertical wall. This is placed between the camera and the enclosure. A cloth is hung from this cardboard aperture and draped over the camera during photography to eliminate camera reflection on the plexiglas. Another larger piece of cardboard covered with white paper is placed 1 foot from the rear small vertical wall to act as a backdrop. Finally a 650 watt colortran multi-6 set lamp is positioned 2 feet from the white cardboard backdrop and 1.5 feet from the apparatus. The lamp is directed towards the white backdrop and turned on only when photographing the flow.

A major concern was that the heat generated by the lamp would disturb the flow. However, due to the insulation remaining between the lamp and the enclosure and the short interval of time the lamp is on the viewed flow remains two dimensional. This scheme provides an excellent view down the length of the enclosure to a white background that adequately contrasts the darkened fluid.

D. DATA ANALYSIS

There are six length dimensions within the enclosure, any one of which could be chosen as the characteristic length, L, for determining the Nusselt number and Rayleigh numbers. The 1.0 inch vertical face of the heater is chosen since it is the surface that not only adds the majority of energy to the system but it also is oriented in the direction of the gravitational driving force of free convection. The properties of the fluid are evaluated at the average of the hot surface (heater) and cold surface (heat exchangers) temperatures.

1. Determination of Nusselt Number

The Nusselt number is defined as follows:

$$Nu = \frac{h\ L}{k_f} \tag{1}$$

To evaluate the heat transfer coefficient an estimate has to be made of the heat lost through the vertical walls of the enclosure. A parallel thermal resistance circuit for conduction through the three vertical walls in contact with the heater is employed for this purpose. Heat loss through the vertical wall opposite the heater, all contact resistances, and conduction via the heater assembly attaching screws are assumed negligible. Knowing the total thermal resistance for conduction the heat loss is calculated using a variation of Fourier's Law of Conduction:

$$Q_{cond} = \frac{T_s - T_a}{R_{cond}} \tag{2a}$$

where

$$R_{cond} = \frac{L}{kA} \tag{2b}$$

The length of the conduction path, L, for all materials is known. The thermal conductivity, k, for each material is determined using a table of properties [22]. The area, A, is assumed to be that of the cartridge heater perpendicular to the conduction path. Finally, the temperature difference is assumed to be the difference between the ambient, T_a, and the heater cover temperature, T_s; this further neglects the convective thermal resistance on the outside of the insulation. In the event T_s is less than T_a, heat loss is assumed to be zero.

After calculating the energy lost via conduction and having already determined the energy into the system (Q_{in}) from the voltage measurements across the heater and the precision resistor a simple energy balance is used to determine the energy convected into the fluid (Q_{conv}):

$$Q_{conv} = Q_{in} - Q_{cond} \tag{3a}$$

where

$$Q_{in} = \frac{V_1 \, V_2}{R} \tag{3b}$$

and

V_1 = voltage across heater
V_2 = voltage across resistor
R = 2.0317 Ohms

Then, using Newton's Law of Cooling,

$$Q_{conv} = h\ A\ (T_s - T_f) \qquad (4)$$

h is calculated. T_f is chosen to be the temperature of the heat exchangers which are the ultimate heat sink for the enclosure. The exterior surface area of the heater cover is A. With all variables in equation (1) now known the Nusselt number is calculated.

To ensure the accuracy of this method of analysis a single iteration is performed on the Nusselt number by use of another thermal resistance for conduction circuit. This time a single circuit with a lone resistance is run through the steel heater cover to the cartridge heater with the intent of determining the cartridge heater temperature. Using the heater cover temperature (T_s), length of the conduction path through the heater cover (L), the thermal conductivity for 304 stainless steel (k_{ss}), the exterior area of the heater cover (A), and the previously calculated convection energy into the enclosure (Q_{conv}), it is a simple matter to determine the cartridge heater temperature (T_h) from a rearrangement of Fourier's Law of Conduction:

$$T_h = \frac{L\ Q_{conv}}{k_{ss}\ A} + T_s \qquad (5)$$

T_s in equation (2a) is then set equal to T_h and a single iteration is performed to re-evaluate the Nusselt number. Iterative analysis of Nusselt numbers for all test runs prove to fall within 3.0% of the initial calculation thus eliminating the necessity for further iterations. A sample calculation is contained in Appendix A.

2. Determination of Rayleigh Number

One definition of the Rayleigh number is as follows:

$$Ra = (Gr)\ (Pr) \tag{6a}$$

where

$$Gr = \frac{g\ \beta\ L^3\ (T_s - T_f)}{\nu^2} \tag{6b}$$

$$Pr = \frac{\nu}{\alpha} \tag{6c}$$

In the calculation of the Grashof number (Gr), the same characteristic length (L) is used as that used to determine the Nusselt number; that is, the 1.0 inch vertical face of the heater cover. In addition, the same temperature difference is used as that in equation (4) (i.e., the average heater cover temperature minus the average heat exchanger temperature). The remaining terms in equation (6b) are evaluated at the average temperature of all thermocouple measurements by a cubic polynomial that had been fit to data from a table of properties [23] for temperatures of water ranging from 50 to 100 degrees Fahrenheit.

The Prandtl number (Pr) is also evaluated by a cubic polynomial that had been fit to data from the same table of properties, at the same temperature, and for the same working fluid. The Rayleigh number is then calculated. A sample calculation is contained in Appendix A. A sample uncertainty calculation is contained in Appendix B.

IV. RESULTS

A. VISUAL

Photographs of the natural convection flow within the enclosure for a representative number of heater locations and Rayleigh numbers are presented in Figs. 6, 7, and 8. Figure 6 depicts flows with the top horizontal face of the heater located 1.0 inches from the top of the enclosure. Figure 7 depicts flows with the heater centered in the enclosure. Finally, Figure 8 depicts flows with the bottom horizontal face of the heater located 1.0 inches from the bottom of the enclosure.

Some general observations can be made about the natural convection flow within the enclosure. First, the flow is dual-celled. There is a buoyancy driven upper cell and a shear driven lower cell. The location of the cell separation layer is dependent upon the heater location within the enclosure; as the heater is raised so, too, is the layer.

Secondly, the flow of the buoyant driven upper cell follows the geometry of the enclosure. The fluid comes off the vertical face of the heater, up the vertical wall to which the heater is attached, across the cold heat exchangers, then down the vertical wall opposite the heater. Finally, the fluid moves along the cell separation layer where it interacts viscously with the lower cell and back towards the

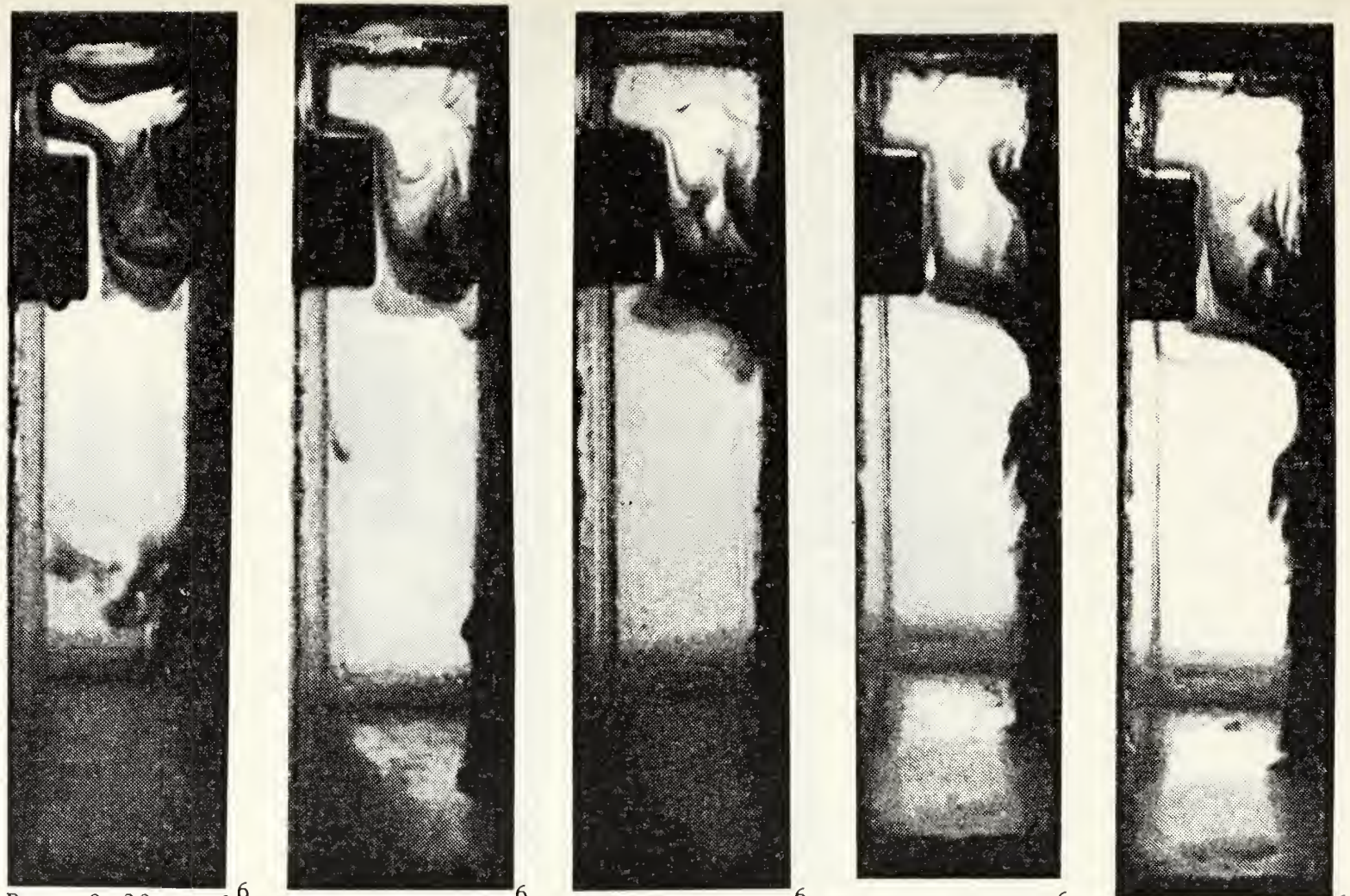

Figure 6. Photographs of Flow with Heater Near Top of Enclosure

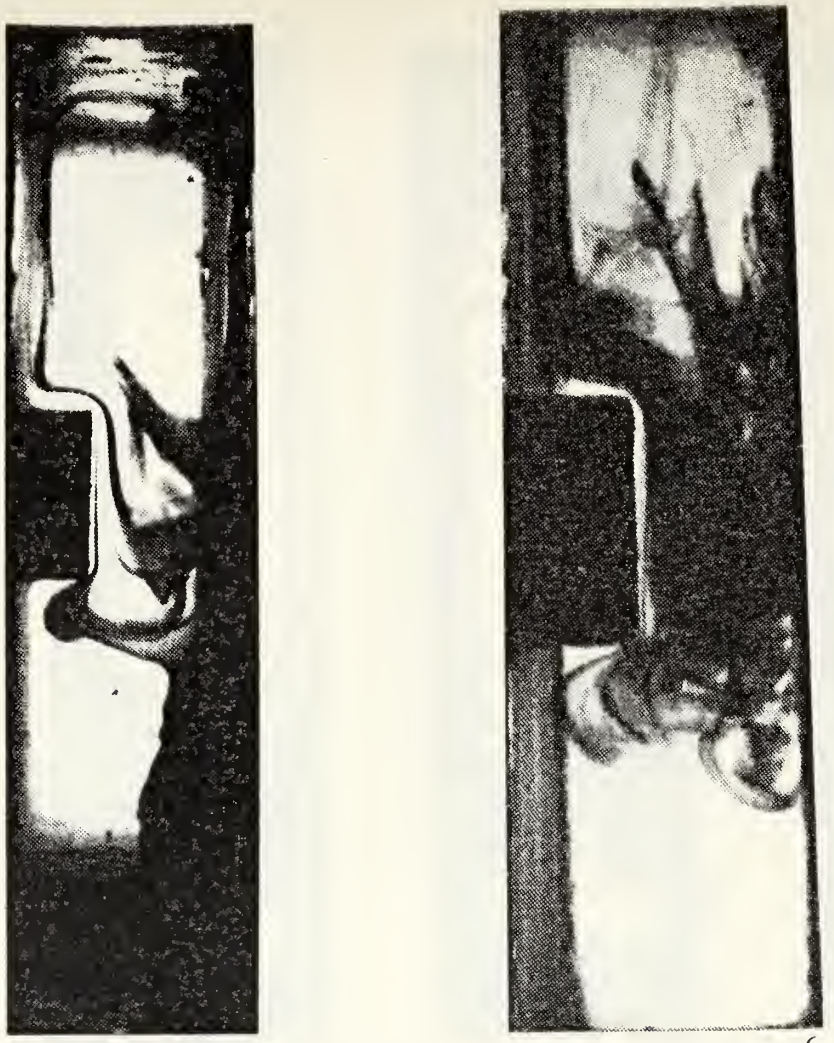

Ra = 0.92×10^6 Ra = 1.09×10^6

Figure 7. Photographs of Flow with Heater Centered in Enclosure

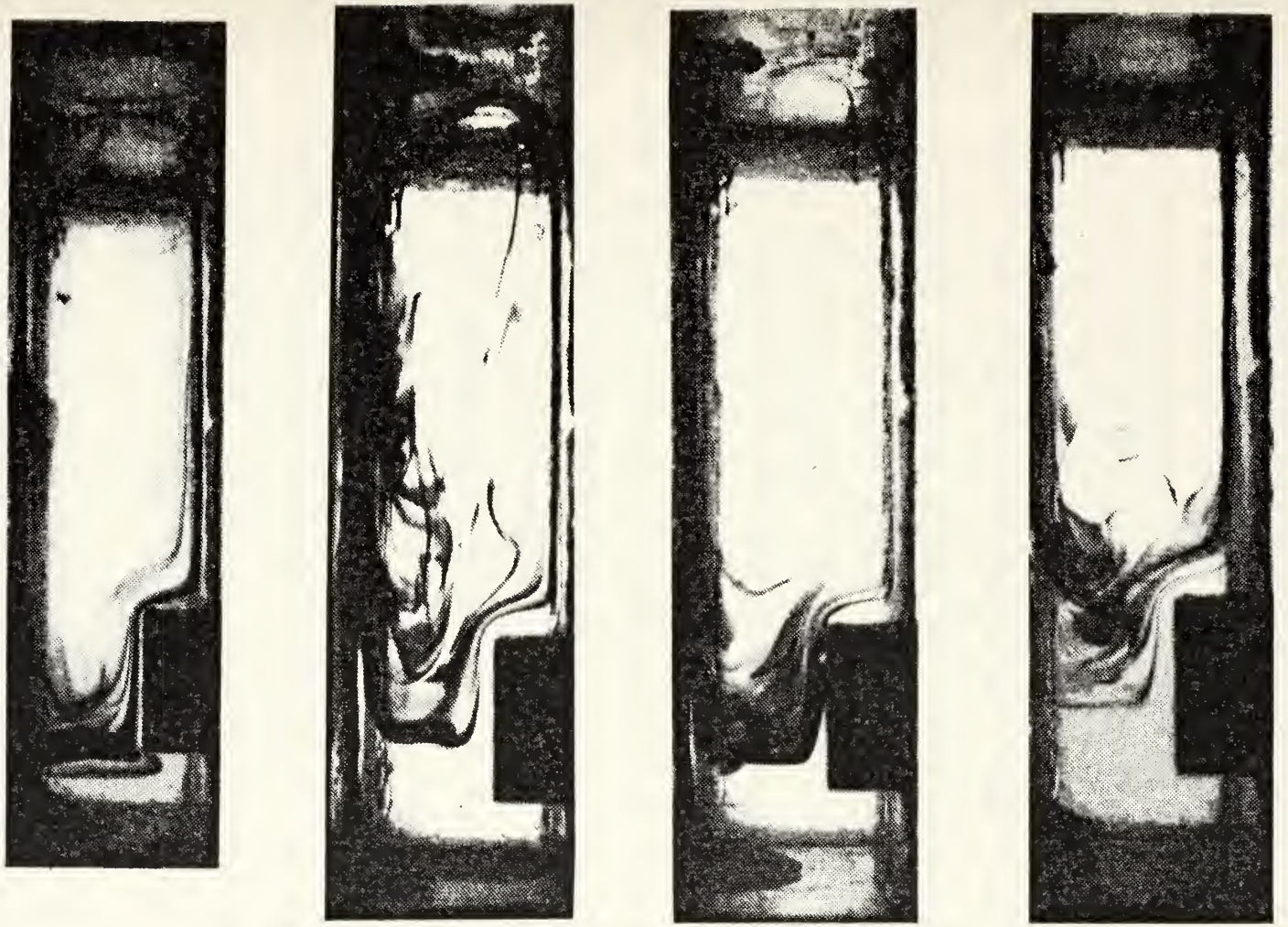

$Ra = 1.13 \times 10^6$ $Ra = 1.4 \times 10^6$ $Ra = 1.7 \times 10^6$ $Ra = 2.7 \times 10^6$

Figure 8. Photographs of Flow with Heater Near Bottom of Enclosure

heater. No definitive comments can be made about the total motion of the fluid in the lower cell; only a very slow moving flow was observed slightly below the separation layer. This flow was crossing the width of the enclosure towards the vertical wall holding the heater.

The photographs also show flow being generated into each cell. This is the result of a recurring problem encountered using the Baker flow visualization technique. Baker suggests applying a maximum of 5.0 volts across the fluid when electrode spacing is 0.5 cm. These limitations preclude generation of bubbles near the cathode. Utilizing the limits imposed and a network of cathodes the ensuing flow can be seen as it moves away from the area of interest. In this experiment a single cathode is used. The area of interest is the entire enclosure. Hence, it is necessary to apply up to 8.0 volts in order to observe the flow throughout the entire enclosure. Bubbles are therefore generated that cause convective mass transfer up the stainless steel shim strip. The buoyant flow circulation of the upper cell collides with the mass transfer associated with the convected bubbles resulting in the intrusion of flow into the cells. Efforts were made to minimize this effect by careful adjustment of the voltage during test runs.

The distinct difference between the photographs of Fig. 7 clearly illustrates the advantage of utilizing a stainless steel shim strip as the cathode for the visualization technique

As previously noted, the heater was originally utilized as the anode while a heat exchanger acted as the cathode. This provided an excellent darkening of the fluid but also proved inadequate in terms of flow visualization (right photograph of Fig. 7). The inclusion of the shim strip as the cathode allows visualization of the two dimensional flow that occurs in the middle of the enclosure (left photograph of Fig. 7).

B. QUANTITATIVE

Table I summarizes the results of calculations using data obtained for each test run. Based on these calculations the Nusselt and Rayleigh numbers were plotted on a log-log graph (Fig. 9). Since the temperature measurement uncertainty inherent in the experiment produces Nusselt and Rayleigh number uncertainties ranging from five to twenty percent (see Appendix II) it is difficult to draw definitive conclusions from the data. However, there does appear to be a trend suggesting that as the heater is raised within the enclosure the Nusselt number decreases.

TABLE I

Summary of Results

T_s (^oF)	T_f (^oF)	Q_{in} (Btu/hr)	Nu	Ra (x 10^6)
Heater Near Top				
65.75	54.00	26.41	4.95	0.99
70.25	50.00	55.75	6.12	1.73
72.25	38.88	102.68	6.84	2.17
81.25	38.88	146.85	7.65	3.61
82.50	39.25	145.52	7.38	3.85
89.75	36.75	197.58*	8.19	5.33
Heater Centered				
66.75	57.00	18.94	4.23	0.92
69.25	59.00	25.99	5.58	1.07
68.50	57.50	28.79	5.76	1.09
69.00	50.50	51.55	6.12	1.55
66.75	42.00	68.15	6.12	1.49
70.50	40.63	99.01	7.38	1.94
70.50	39.25	103.80	7.38	1.95
77.75	39.75	144.89	8.46	3.00
75.50	36.75	147.37	8.46	2.61
79.00	39.50	147.33	8.28	3.21
80.00	39.25	148.06	8.01	3.38
88.00	40.00	185.42*	8.46	5.01
99.50	38.00	248.91*	8.73	7.95
Heater Near Bottom				
68.25	56.50	28.78	5.40	1.13
68.00	51.00	51.24	6.66	1.40
68.50	40.00	98.12	7.74	1.70
75.75	40.00	139.54	8.64	2.68

Note: (1) * indicates Variac used as power supply

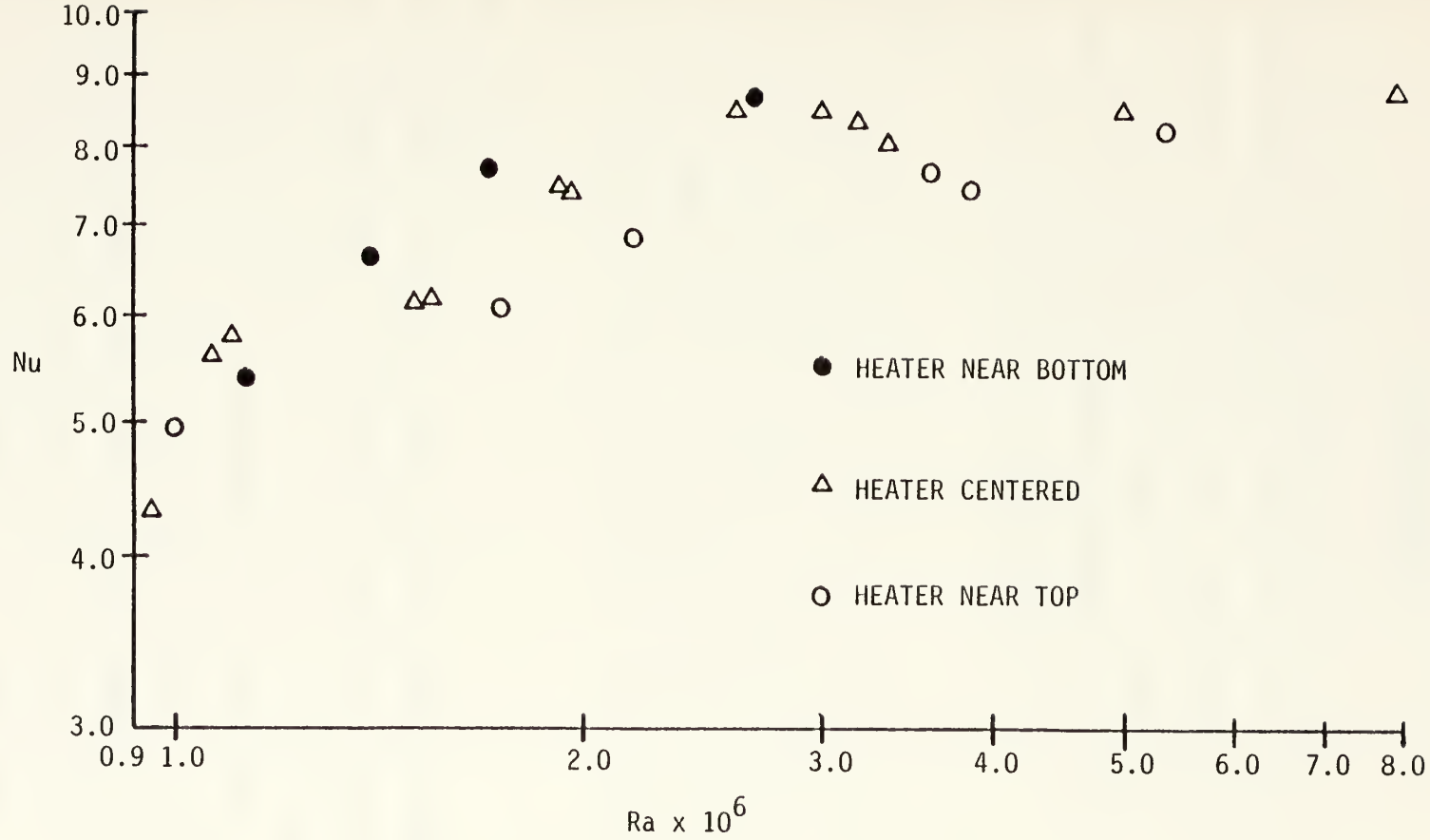

Figure 9. Data Plot of Nusselt versus Rayleigh Number

V. CONCLUSIONS

The author has found no previous natural convection study of a liquid filled rectangular enclosure with a heated protrusion attached to a vertical wall, temperature variant horizontal walls, and the remaining walls adiabatic. However, some investigators using similar configurations have reached the same conclusions about to be presented.

A. VISUAL

Two cells occur within the enclosure during the natural convection flow. The upper cell is driven by buoyant forces and essentially follows the geometry of the enclosure. The lower cell is shear driven. The location of the cell separation layer is dependent upon the height of the heater in the enclosure.

B. QUANTITATIVE

Calculations indicate a trend for the Nusselt number to decrease as the height of the heater within the enclosure is increased. It is interesting to note that for the Rayleigh numbers calculated in this experiment (on the order of 10^5 to 10^6) Chu, et al [11] plot this same tendency for an air filled square enclosure that has a heater imbedded in a vertical wall and cooled horizontal walls. It is Chu's investigation that most closely resembles this experiment.

VI. RECOMMENDATIONS

A. IMPROVEMENT TO EXPERIMENT

1. Apparatus

Fluid leakage into the heater assembly occurred during the course of the experiment. This caused the cartridge heater to fail. Replacement of the cartridge heater necessitated dismantling the apparatus. To avoid the problem of cartridge heater malfunction, either a liquid immersible cartridge heater should be used or else an improved design of the heater cover should be sought.

Though the photographs proved satisfactory it is further suggested that experimentation with various camera filters be done. The contrast of the observed flow may improve to the point where excessive voltage across the fluid may not be required, thereby, eliminating the bubble generation effect.

2. Instrumentation

In order to lower the experimental uncertainty it is suggested that a more accurate temperature measuring instrument be used for thermocouple readings. Further, to preclude the use of the Variac transformer a cartridge heater with the same power (180 watts) but rated at 60 instead of 120 volts should be used. This will allow all test runs to be made with the Lambda power supply as the power supply to the heater.

B. ADDITIONAL EXPERIMENTAL WORK

It is suggested that the following areas of study be experimentally explored:

1. Decrease the enclosure width to see if any additional cells develop within the enclosure.

2. Observe the effects of independently varying the heat exchanger temperatures. In conjunction with this, do not allow the coolant temperature to go below fifty degrees Fahrenheit to avoid the density inversion that occurs in water at forty degrees. As can be seen in Table I, the heat exchanger temperatures for some test runs fell below this value.

3. Continue to use the stainless steel shim strip as the cathode but seek methods of decreasing the effect of the bubbles generated when voltage is applied across the fluid. Alternatively, design a network of cathodes (as suggested by Baker) that encircles the enclosure.

APPENDIX A: SAMPLE CALCULATIONS

A. DETERMINATION OF INPUT POWER

The dimensions of the cartridge heater are 8.0 by 0.25 by 0.725 inches. Table II is the data that was recorded for a representative run on 3 November 1983 with the heater located near the bottom of the enclosure. Refer to Fig. 1 for thermocouple locations.

TABLE II

Test Run Data for 3 November 1983

T_1	T_2	T_3	T_4	T_5	T_6	T_7	T_8	T_a	V_1	V_2
40	40	40	40	73	77	77	76	71	58.51	1.42

Notes: (1) all temperatures in degrees Fahrenheit
(2) all voltages in volts

Using equation 3b the input power is calculated to be:

$$Q_{in} = \frac{(58.51)\ (1.42)}{(2.0317 \text{ ohms})}\ (3.4123 \text{ Btu/hr-Watt}) = 139.54 \text{ Btu/hr}$$

B. NUSSELT NUMBER

The heat loss via conduction through the vertical walls is determined by constructing a thermal resistance network

(Fig. 10). The thermal conductivity of each material (Table III) is determined from a table of properties [22].

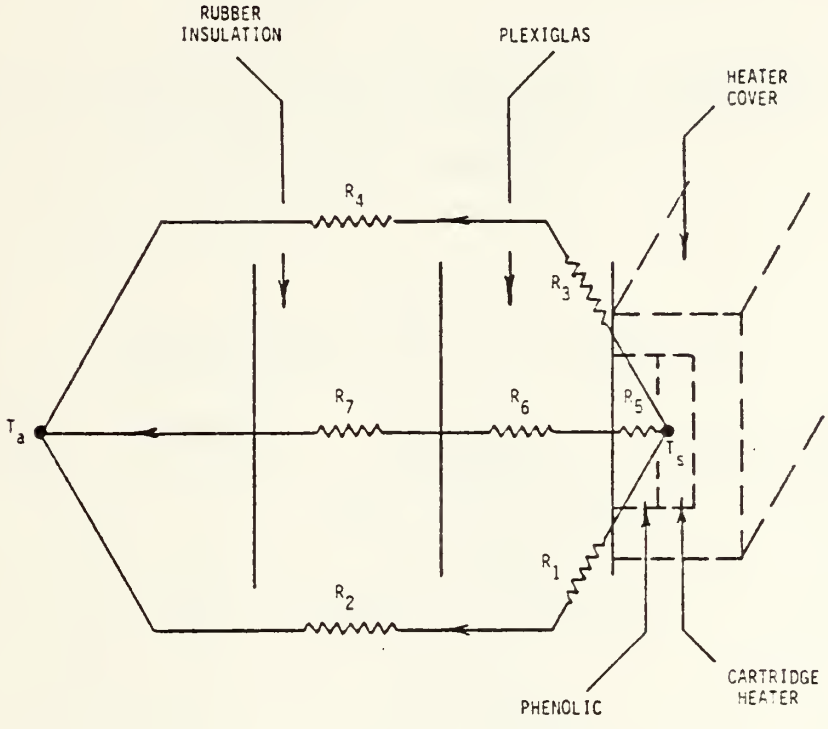

Figure 10. Thermal Resistance Network for Calculation of Losses

TABLE III

Thermal Conductivity of Materials

Material	K (Btu/hr-ft-^{o}F)
rubber insulation	0.0225
plexiglas	0.0821
phenolic	0.0173
304 steel	8.8693

Table IV is a summary of the individual resistances for Fig. 10 that were determined using equation 2b.

TABLE IV

Thermal Resistances to Conduction

Resistance	Path(1)	Material	Value (^{o}F-hr/Btu)
R_1	a	plexiglas	116.9
R_2	a	rubber insulation	2562.7
R_3	b	plexiglas	643.2
R_4	b	rubber insulation	2562.7
R_5	c	phenolic	8.7
R_6	c	plexiglas	20.1
R_7	c	rubber insulation	80.1

Note: (1) conduction path through
a. viewing wall
b. wall opposite viewing
c. wall to which heater is attached

The equivalent resistance for each path is:

$$R_a = 2679.6 \quad {}^{o}F\text{-hr/Btu}$$

$$R_b = 3205.9 \quad {}^{o}F\text{-hr/Btu}$$

$$R_c = 108.8 \quad {}^{o}F\text{-hr/Btu}$$

Therefore,

$$R_{cond} = \frac{(R_a)\ (R_b)\ (R_c)}{(R_a)(R_b)+(R_a)(R_c)+(R_b)(R_c)} = 101.28\ {}^{o}F\text{-hr/Btu}$$

Employing equation 2a,

$$Q_{cond} = \frac{(75.75 - 40.0)}{(101.28)} = 0.047 \quad \text{Btu/hr}$$

The Nusselt number is determined by first using equation 3a to calculate the energy convected into the fluid:

$$Q_{conv} = (139.54 - 0.047) = 139.495 \quad \text{Btu/hr}$$

Then, the heat transfer coefficient is calculated as (equation 4)

$$h = \frac{(139.495)\ (144)}{(75.75-40.0)(16)} = 35.10\ \text{Btu/hr-ft}^2\text{-}{}^{o}F$$

The thermal conductivity of water is determined from a table of properties [23],

$$k_f = 0.3383 \quad \text{Btu/hr-ft-}^{o}\text{F}$$

Finally, the Nusselt number can be calculated (equation 1),

$$Nu = \frac{(35.10)\ (1/12)}{(0.3383)} = 8.64$$

An iterative check is performed by determining the cartridge heater temperature (equation 5) as

$$T_h = \frac{(3/192)\ (139.495)}{(8.659)\ (1.33)} + 75.75 = 77.96\ ^{o}\text{F}$$

Reapplication of equations 2a, 3a, 4, and 1 respectively with T_s set equal to T_h yields

$$Q_{cond} = \frac{(77.96 - 71.0)}{(101.285)} = 0.0687 \quad \text{Btu/hr}$$

$$Q_{conv} = (139.54 - 0.0687) = 139.474 \quad \text{Btu/hr}$$

$$h = \frac{(139.474)\ (144)}{(77.96 - 71.0)(16)} = 35.10 \quad \text{Btu/hr-ft}^2\text{-}^{o}\text{F}$$

From the table of properties [23] the fluid conductivity remains

$$k_f = 0.3383 \quad \text{Btu/hr/ft/}^{o}\text{F}$$

Therefore,

$$Nu = \frac{(35.10)\ (1/12)}{(0.3383)} = 8.64$$

The percent difference in Nusselt numbers after one iteration is zero percent.

C. RAYLEIGH NUMBER

Using the property table [23] at the average temperature of the heater and heat exchangers the Prandtl number and Grashof number can be calculated as:

$$Pr = 8.322$$

$$\frac{g\beta}{\nu^2} = 15.58 \times 10^6\ 1/^oF/\text{cubic ft}$$

$$Gr = (15.58)\ (77.96 - 40.0)\ (1/1728) = 322.4 \times 10^3$$

Therefore, the Rayleigh number can be determined using equation 6a:

$$Ra = (322.4 \times 10^3)\ (8.322) = 2.683 \times 10^6$$

APPENDIX B: UNCERTAINTY ANALYSIS

Uncertainties in the experiment are evaluated by employing the root mean square method of Kline and McClintock [24]. Table V is a summary of measurement and property values and their associated uncertainties:

TABLE V

Uncertainty in Variables

Variable	Uncertainty	Basis for Uncertainty
$g\beta/\nu^2$	1/250	assume last digit
k_f	1/300	assume last digit
k_g	5.0 %	[22]
k_i	7.0 %	[22]
k_p	7.0 %	[22]
k_{ss}	5.0 %	[22]
L (1)	0.001 in	resolution of measurement device
Pr	1/600	assume last digit
R	0.0001 ohms	calibration on galvonometer
T (2)	1.0 F	resolution of measurement device
V_1(3)	0.01 volts	resolution of measurement device
V_1(4)	2.0 volts	resolution of measurement device
V_2	0.01 volts	resolution of measurement device

Notes: (1) all dimension measurements
(2) all thermocouple temperature measurements
(3) Lambda regulator as power supply
(4) Variac as power supply

The following variable uncertainties are determined using the aforementioned RMS equation on the data presented in Table II of Appendix A.

$$WQ_{in} = \left[\left(\frac{(WV_1)(V_2)}{R}\right)^2 + \left(\frac{(WV_2)(V_1)}{R}\right)^2 + \left(\frac{(WR)(V_1)(V_2)}{R}\right)^2\right]^{1/2}$$

$$= \left[\left(\frac{(0.01)(1.42)}{(2.0317)}\right)^2 + \left(\frac{(0.01)(58.51)}{(2.0317)}\right)^2 + \left(\frac{(0.0001)(58.51)(1.42)}{(2.0317)^2}\right)^2\right]^{1/2}$$

$$= 0.983 \quad \text{Btu/hr}$$

$$WQ_{cond} = \left[\left(\frac{WT_s}{R_{cond}}\right)^2 + \left(\frac{WT_a}{R_{cond}}\right)^2 + \left(\frac{(WR_{cond})(T_a - T_s)}{(R_{cond})^2}\right)^2\right]^{1/2}$$

$$= \left[\left(\frac{(2)(1/2)}{(101.28)}\right)^2 + \left(\frac{(2)(1/2)}{(101.28)}\right)^2 + \left(\frac{(0.00005)(2)}{(101.28)^2}\right)^2\right]^{1/2}$$

$$= 6.017 \quad \text{Btu/hr}$$

$$WQ_{conv} = \left[(WQ_{cond})^2 + (WQ_{in})^2\right]^{1/2}$$

$$= \left[(0.017)^2 + (0.983)^2\right]^{1/2}$$

$$= 0.983 \quad \text{Btu/hr}$$

$$WNu = \left[\left(\frac{(Wh)(L)}{(k_f)}\right)^2 + \left(\frac{(WL)(h)}{(k_f)}\right)^2 + \left(\frac{(Wk_f)(h)(L)}{(k_f)^2}\right)^2\right]^{1/2}$$

$$= \left[\left(\frac{(2.95)(0.083)}{(0.338)}\right)^2 + \left(\frac{(0.001)(35.10)}{(0.338)}\right)^2 + \left(\frac{(0.001)(35.10)(0.083)}{(0.338)^2}\right)^2\right]^{1/2}$$

$$= 0.727$$

$$WRa = \left[((WGr)(Pr))^2 + ((WPr)(Gr))^2\right]^{1/2}$$

$$= \left[((21.0 \times 10^3)(8.322))^2 + ((0.0)(322.0 \times 10^3))^2\right]^{1/2}$$

$$= 178.85 \times 10^3$$

The above uncertainty calculations are intended to be representative of the method used; calculations performed on every variable are not included. A summary of quantitative results for Nusselt and Rayleigh numbers and their respective uncertainties in relation to heater temperature minus exchanger temperature for all test runs is given in Table VI.

TABLE VI

Uncertainty in Experiment

$T_s - T_f$	Nu	% Uncertainty	Ra (x 10^6)	% Uncertainty
Heater Near Top				
11.75	4.95	18.20	0.99	17.40
20.25	6.12	11.73	1.78	10.52
33.38	6.84	8.69	2.17	7.00
42.38	7.65	7.85	3.61	5.95
43.25	7.38	7.79	3.85	5.88
53.00*	8.19	7.89	5.33	5.23
Heater Centered				
9.75	4.23	21.57	0.92	20.83
10.25	5.58	20.55	1.07	19.85
11.00	5.76	19.28	1.09	18.53
18.50	6.12	12.53	1.55	11.40
24.75	6.12	10.26	1.49	8.86
29.88	7.38	9.19	1.94	7.61
31.25	7.38	8.97	1.95	7.35
38.00	8.46	8.19	3.00	6.39
38.75	8.46	8.13	2.61	6.31
39.50	8.28	8.07	3.21	6.23
40.75	8.01	7.97	3.38	6.10
48.00*	8.46	8.07	5.01	5.52
61.50*	8.73	7.53	7.95	4.87
Heater Near Bottom				
11.75	5.40	18.19	1.13	17.40
17.00	6.66	13.37	1.40	12.31
28.50	7.74	9.43	1.70	7.90
35.75	8.64	8.41	2.68	6.67

Note: (1) * Indicates Variac used as power supply.

LIST OF REFERENCES

1. Solomon, S., "The Idaho Chip," Science Digest, v. 91, No. 7, p. 16, July 1983.

2. Report of Research Workshop, NSF Grant ENG-7701297, Directions of Heat Transfer in Electronic Equipment, by R. C. Chu, 1977.

3. Hannemann, R., "Electronic System Thermal Design for Reliability," IEEE Transactions on Reliability, v. R-26, No. 5, pp. 306-310, December 1977.

4. Kraus, A. D., Chu, R. C., and Bar-Cohen, A., "Thermal Management of Microelectronics: Past, Present, and Future," Computers in Mechanical Engineering, pp. 69-79, October 1982.

5. Bar-Cohen, A., Kraus, A. D., and Chu, R. C., "Thermal Frontiers in the Design and Packaging of Microelectronic Equipment," Mechanical Engineering, pp. 53-59, June 1983.

6. Bergles, A. E., Chu, R. C., and Seely, J. H., Survey of Heat Transfer Techniques Applied to Electronic Equipment, paper presented at National Electronic Packaging and Production Conference, 1977.

7. Simons, R. E., and Moran, K. P., Immersion Cooling Systems for High Density Electronic Packages, paper presented at National Electronic Packaging and Production Conference, May 1977.

8. Kraus, A. D., and Bar-Cohen, A., Thermal Analysis of Electronic Equipment, pp. 377-408, Hemisphere Publishing Corporation, 1983.

9. Wilkes, J. O., and Churchill, S. W., "The Finite-Difference Computation of Natural Convection in a Rectangular Enclosure," A.I.Ch.E.Jl, v. 12, pp. 161-166, 1966.

10. Szekely, J. and Todd, M. R., "Natural Convection in a Rectangular Cavity Transient Behavior and Two Phase Systems in Laminar Flow," Int. J. Heat Mass Transfer, v. 14, pp. 467-482, 1971.

11. Chu, H. H-S, Churchill, S. W., and Patterson, C. V. S., "The Effect of Heater Size, Location, Aspect Ratio, and Boundary Conditions on Two-Dimensional, Laminar, Natural Convection in Rectangular Channels," Journal of Heat Transfer, pp. 194-201, May 1976.

12. Markatos, N. C., and Pericleous, C. A., "Laminar and Turbulent Natural Convection in an Enclosed Cavity," Natural Convection in Enclosures - 1983, HTD-Vol. 26, ASME Publication, pp. 61-68, 1983.

13. Megerlin, F. E., and Vingerhoet, P., "Thermal Control of Densely Packaged Microelectronics in Dielectric Fluids," IEEE NAECON, pp. 254-259, 1971.

14. Nansteel, M. W., and Greif, R., "Natural Convection in Undivided and Partially Divided Rectangular Enclosures," Journal of Heat Transfer, v. 103, pp. 623-629, November 1981.

15. Baker, E., "Liquid Immersion Cooling of Small Electronic Devices," Microelectronics and Reliability, v. 12, pp. 163-173, 1973.

16. Lin, Y-S, Akins, R. G., "An Experimental Study of Flow Patterns and Heat Transfer by Natural Convection Inside Cubical Enclosures," Natural Convection in Enclosures - 1983, HTD-Vol. 26, ASME Publication, pp. 35-42, 1983.

17. Ostrach, S., Loka, R. R., and Kumar, A., Natural Convection in Low Aspect-Ratio Rectangular Enclosures, paper presented at National Heat Transfer Conference, 1-10 July 1980.

18. Bohn, M. S., and Kirkpatrick, A. T., "High Rayleigh Number Natural Convection in an Enclosure Heated from Below and from the Sides," Natural Convection in Enclosures - 1983, HTD-Vol. 26, ASME Publication, pp. 27-33, 1983.

19. Catton, I., "Natural Convection in Enclosures," Sixth International Heat Transfer Conference Keynote Papers, v. 6 pp. 13-32, Hemisphere Publishing Corporation, August 1978.

20. Baker, D. J., "A Technique for the Precise Measurement of Small Fluid Velocities," J. Fluid Mech, v. 26, pp. 573-575, 1966.

21. O'Conner, J. M., Natural Convection Flow Visualization and Heat Transfer from a Horizontal Circular Disk, M.S. Thesis, Naval Postgraduate School, Monterey, California, June 1974.

22. Touloukian, Y. S., and others, Thermophysical Properties of Matter, vols. 1 and 2, I F I/Plenum, 1970.

23. Kreith, F., Principles of Heat Transfer, Intext Education Publishers, p. 638, 1973.

24. Kline, S. J. and McClintock, F. A., "Describing Uncertainties in Single-sample Experiments," Mech. Eng. p. 3, January 1953.

INITIAL DISTRIBUTION LIST

		No. Copies
1.	Defense Technical Information Center Cameron Station Alexandria, Virginia 22314	2
2.	Library, Code 0142 Naval Postgraduate School Monterey, California 93943	2
3.	Professor M. D. Kelleher, Code 69Kk Department of Mechanical Engineering Naval Postgraduate School Monterey, California 93943	1
4.	Department Chairman, Code 69 Department of Mechanical Engineering Naval Postgraduate School Monterey, California 93943	1
5.	LCDR Rick H. Knock Code 69 Naval Postgraduate School Monterey, California 93943	1

207040

Thesis
K657
c.1

Knock
Flow visualization study of natural convection from a heated protrusion in a liquid filled rectangular enclosure.